

## Transformation cosmology

Huanyang Chen,<sup>1,\*</sup> Sicen Tao,<sup>1</sup> Jakub Bělin,<sup>2,†</sup> Johannes Courtial,<sup>2,†</sup> and Rong-Xin Miao<sup>3</sup>

<sup>1</sup>*Institute of Electromagnetics and Acoustics and Key Laboratory of Electromagnetic Wave Science and Detection Technology, Xiamen University, Xiamen 361005, China*

<sup>2</sup>*School of Physics & Astronomy, College of Science & Engineering, University of Glasgow, Glasgow G128QQ, United Kingdom*

<sup>3</sup>*School of Physics and Astronomy, Sun Yat-Sen University, 2 Daxue Road, Zhuhai 519082, China*



(Received 14 August 2019; accepted 14 July 2020; published 24 August 2020)

Recent observation of black hole and gravitational wave has stirred up great interest in Einstein's general relativity. In an optical system, the "optical black hole" has also been a key topic in mimicking black holes. Another good way to study or mimic general relativity effects is based on transformation optics. In this paper, we propose a way by utilizing transformation optics theory to directly obtain the equivalent isotropic refractive index profiles which are the analogies of some static spaces of general relativity, such as de Sitter space, anti-de Sitter space, and Schwarzschild black hole. We find that the analog of de Sitter space is the Poincaré disk, while anti-de Sitter space is equivalent to Maxwell's fish-eye lens. In particular, we prove that the optical black hole actually has infinite number of photon spheres, while our black hole only has a single one, which is closer to the real black hole. We study the effect from both geometric optics and wave optics. It can also be generalized to mimic any kind of metrics. Furthermore, with the isotropic refractivity index profile, we visualize the gravitational lensing effect of black hole from our software Dr TIM. The image not only recovers the donutlike halo of black hole, but also shows other phenomena.

DOI: [10.1103/PhysRevA.102.023528](https://doi.org/10.1103/PhysRevA.102.023528)

### I. INTRODUCTION

Einstein's general relativity [1] is actively recalled recently as it well predicted gravitational wave [2] and black hole [3] that were lately observed. Besides, it would be fantastic if the celestial mechanics could be mimicked in laboratories. A novel method is called general relativity in electrical engineering [4], which could be used to mimic similar cosmic phenomena by complicated electromagnetic material parameters, like that from transformation optics [5–7]. Transformation optics, thanks to its convenience and flexibility on manipulating electromagnetic waves, has a great many applications, including, but not limited to invisibility cloaks [5,6], rotators [8,9], concentrators [10,11], perfect lenses [12,13], and electromagnetic cavities [14]. In addition, as mentioned before, optical analogs of general relativity effects demonstrated by four-dimensional (4D) metrics have been designed. For example, a simulation of a derived permittivity tensor profile and a permeability has been proved to be equivalent to a Schwarzschild black hole [15]. A generalized analytical formalism for developing analogs of spherically symmetric static black holes was discussed [16]. The equivalent time-dependent material parameters can be used to achieve the cosmological redshift [17]. Other works, such as to mimic de Sitter space [18,19], time travel effect [20], have also been proposed based on this electrical general relativity [4]. However, this method requires complicated material parameters, thereby making experiments difficult to implement. Although

uniaxial medium for Schwarzschild–(anti-)de Sitter space-time could be obtained by constructing the Tamm medium which constitutes simple homogenized component parameters, there still exist many restrictions and tedious processes [21]. Nevertheless, by performing transformation optics [22], the complicated parameters could be simplified into isotropic refractive index profiles [23], which not only make calculation simpler [24], but also make experiment more feasible, such as the black holes in microwave [25] and visible frequencies [26]. Other general relativity effects, such as Einstein's ring [27] and cosmic string [28], have also been mimicked for visible frequencies.

On the other hand, the topic of mimicking black hole has been studied for a long time. The "optical black hole" [23] has a good absorption efficiency. Finite-difference time-domain calculation method has been used to prove the absorption property [24]. The corresponding experiment results [25] also show great agreement with the theoretical work [23]. However, we will prove that this optical black hole actually contains infinite number of photon spheres. It is exactly rather a light absorber than a black hole, while our black-hole model which carries only one photon sphere shows more similarity with the realistic black hole.

In this paper, we come up with some spatial mappings, combining the metric formulas, to get the isotropic material parameters. We will show the analog spaces (de Sitter space and black hole) both in geometric optics and in wave optics. We will prove that the equivalent spaces of de Sitter space and anti-de Sitter space are exactly the Poincaré disk and Maxwell's fish-eye lens, respectively. Moreover, visualization of black hole will be demonstrated. It reveals the details outside the event horizon and gives us a more intuitional

\*kenyon@xmu.edu.cn

†Johannes.Courtial@glasgow.ac.uk

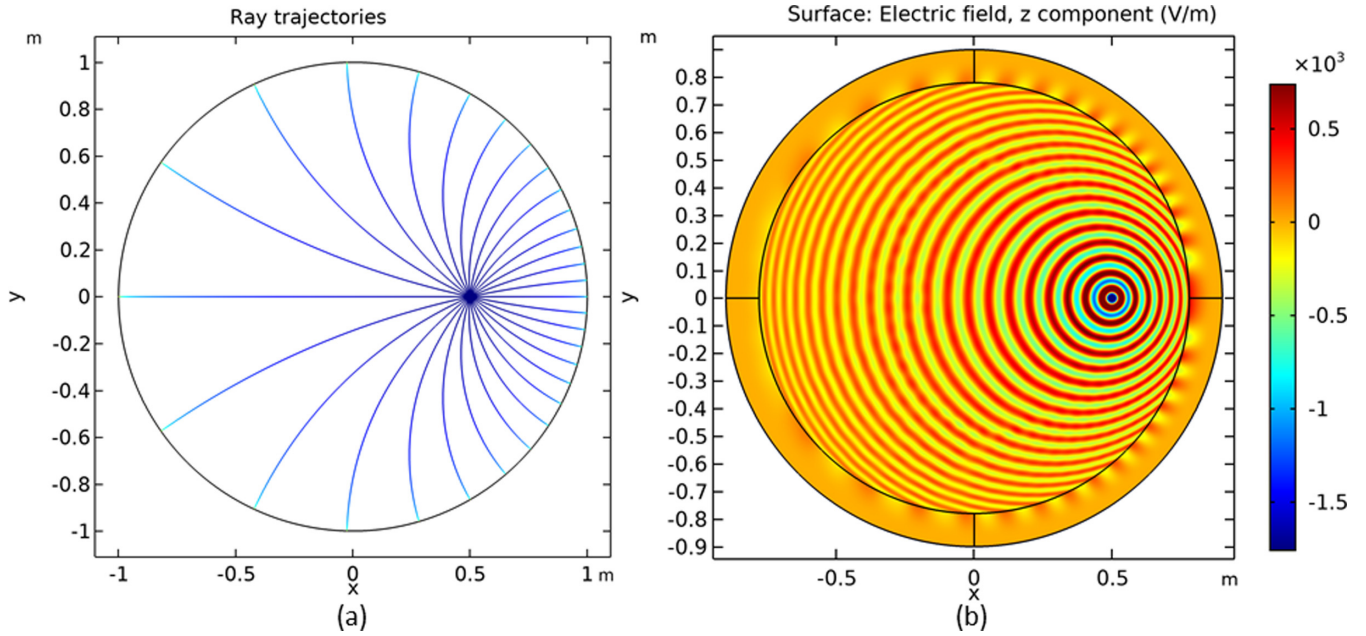


FIG. 1. A point source inside the de Sitter profile [Eq. (5)]: (a) the ray trajectories; (b) the field pattern.

image of gravitational lensing effect around the event horizon. Our black-hole model has only one photon sphere, so that we could see the donutlike halo of black hole. It should be noted that our model contains only spatial transformation without considering the time dimension. That is, we are just concerned about the space change of three-dimensional (3D) optical metric. Therefore, we do not need to worry about the causal structure's swapping in 4D manifold of space-time [29,30]. Furthermore, we believe that, compared with anisotropic material parameters, the isotropic refractive index profiles can be easier to fabricate. For instance, the geodesic lenses give us some hints on investigating light propagation on curved surfaces that can be connected to this kind of refractive index profile [31,32].

## II. CALCULATION AND RESULTS

We start from a general metric form of

$$ds^2 = -f(r)dt^2 + \frac{1}{f(r)}dr^2 + r^2d\Omega^2. \quad (1)$$

In this paper, we will show that such a metric form could be equivalent to a refractive index profile by transformation optics. With this method, experimental realization becomes much easier and simulations of ray-optical phenomena can be performed in custom ray tracers, e.g. Dr TIM [33].

We perform a mapping in the radial direction  $r = r(R)$  (or  $R = R(r)$ ); the metric is then transformed into the following form:

$$ds^2 = -f(r(R))dt^2 + \frac{dr^2/dR^2}{f(r(R))}dR^2 + \frac{r^2}{R^2}R^2d\Omega^2. \quad (2)$$

To obtain a spacial isotropic metric, we should let [22]

$$\frac{dr^2/dR^2}{f(r(R))} = \frac{r^2}{R^2}, \quad (3)$$

which could be used to obtain the required mapping by considering suitable boundary condition. After that, it would be easy to get the equivalent refractive index profile [22],

$$n(R) = (g/g_{00})^{1/2} = \frac{|dr(R)/dR|}{f(r(R))} = \frac{r(R)}{R\sqrt{f(r(R))}}. \quad (4)$$

The inverse process is also very interesting. Given the refractive-index profile, one can solve Eq. (4) for  $f(r)$  to get a corresponding space-time metric, whose form is given by Eq. (1), although such a metric is not exactly a solution of Einstein's field equations.

For example, when  $f(r) = 1 - \frac{r^2}{a^2}$  ( $r \leq a$ , the horizon), the metric is for de Sitter space. After the mapping of  $r = \frac{2R}{1 + \frac{R^2}{a^2}}$ , according to Eq. (4), the equivalent refractive index profile should be

$$n(R) = \frac{2}{1 - \frac{R^2}{a^2}} \quad (\text{for } R \leq a, \text{ the transformed horizon}). \quad (5)$$

Using the commercial software COMSOL MULTIPHYSICS as the simulation tool, Fig. 1(a) shows light rays emerging from a point source, situated at an arbitrary point inside the space. All the emitted rays become perpendicular to the horizon  $R = a$ . Actually, Eq. (5) is exactly the Poincaré disk metric. The geometry of the Poincaré disk is limited in a unit disk, in which straight lines consist of all circular arcs that are orthogonal to the boundary of the disk [34,35]. It means that light will never reach the boundary and anyone, wherever he or she is in such a space, will always be the center of the universe. This is an inverse effect of a black hole, which will be further analyzed in a later section. We also plot the field pattern in wave optics in Fig. 1(b). For simplicity, we performed the above simulations in two-dimensional cylindrical coordinate system, because it has the same optical behaviors as that in three dimensions and is easier to simulate or realize in table-top devices. It should be noted that in wave-optics perspective we set the boundary

radius a little bit smaller than  $a$  (here it is 1) to avoid reaching the singularity of the horizon and to better perform the field pattern. A perfectly matched layer was added to truncate the space. This profile will change the cylindrical wave front from any point into a cylindrical wave front with its center at the origin when approaching the horizon, which is also similar to the zero index lens [36].

When  $f(r) = 1 + \frac{r}{a^2}$ , the metric is for anti-de Sitter space. After the mapping of  $r = \frac{2R}{1 - \frac{R^2}{a^2}}$ , the equivalent refractive index profile should be

$$n(R) = \frac{2}{1 + \frac{R^2}{a^2}}, \quad (6)$$

which is the famous Maxwell's fish-eye lens [37], a perfect lens with positive refraction. Similar process could be

$$n(R) = \frac{(R + \frac{L}{4})^3}{R^2(R - \frac{L}{4})} (1 + i) \quad \left( \text{for } R < \frac{L}{4}, \text{ the transformed horizon} \right). \quad (8)$$

It reminds us of the interior of black hole [39,40], which is exact solution of Einstein's field equation. It could help us better understand the black hole with a viewpoint of an observer inside the event horizon, and make the research more complete. In this paper, we will pay more attention to the studies outside the black hole and not go into details of the inner core; we use Eq. (8) above as an absorber for our black hole. Nevertheless, the interior of black hole is still an interesting topic for future research, as the interior structure of realistic black holes have not been satisfactorily determined, and are still open to considerable debate, as stated in Ref. [39].

We will prove that the profile of Eq. (7) indeed mimics a Schwarzschild black hole. Before we get into the details, let us recall the isotropic black hole that is usually used in metamaterials [23]. The profile is

$$n(R) = \frac{1}{R} \quad (\text{for } R \geq L_0, \text{ the horizon}). \quad (9)$$

This could also be obtained from conformal transformation optics [5,41], with  $n_z = n_w |\frac{dw}{dz}|$  for  $n_w = 1$  and  $w = \ln z$  [42], where  $R = |z|$  and  $n_z = n(R)$ . For any  $R \geq L_0$ , light will travel in circles, as it is mapped to the real coordinate of  $w$ . In other words, such a profile will have infinite numbers of photon spheres. However, for the profile in Eq. (7), the unique photon sphere is at  $R = (2 + \sqrt{3})\frac{L}{4}$ , which is mapped from  $r = \frac{3L}{2}$  (see Appendix A). In Fig. 2(a), we put a point source at the photon sphere. We find that part of the rays will escape from the black hole, and part will be trapped by the photon sphere and approach the horizon perpendicularly. In fact, for the rays that emit to the left direction, which is under the photon sphere, they will all be trapped and incident on the event horizon perpendicularly, while for the rays that emit to the right direction, which is outside the photon sphere, they will all be bent and escape the event horizon. We also plot the field pattern in wave optics for a point source in Fig. 2(b). The waves will interfere with each other at the opposite site of the source. The same trick was used here that we make

performed for any  $f(r)$ , which is very promising to study various metrics in laboratories. In the paper, we hope to recall the black hole in Ref. [15], where  $f(r) = 1 - \frac{L}{r}$  ( $r \geq L$ , the horizon). A similar trick suggests the mapping of  $r = \frac{(R + \frac{L}{4})^2}{R}$ , which was also called an isotropic radial coordinate transformation [38], and the equivalent refractive index profile should be

$$n(R) = \frac{(R + \frac{L}{4})^3}{R^2(R - \frac{L}{4})} \quad \left( \text{for } R \geq \frac{L}{4}, \text{ the transformed horizon} \right). \quad (7)$$

Here, similar to the previous work [15,23], we take the following parameters for the inner core. The imaginary part works as a loss term to absorb the fields at the event horizon.

the radius of horizon slightly larger in wave simulations than  $\frac{L}{4}$  (here  $L$  is 1) to better present the field pattern and prevent wave approaching the singularity of the event horizon. The same way is applied to Fig. 2(d).

It is because of the photon sphere that we could see the donutlike halo from the earth [3]. We therefore study the case of parallel light rays incident to the black hole in Fig. 2(c). For rays outside the photon sphere, they will be bent due to the gravitational lens effect of the black hole. For the rays incident almost tangential to the photon sphere, they will propagate in a U-turn trajectory, just like the Eaton lens [43,44]. For the rays impinging at the photon sphere, they will all be trapped and approach the horizon perpendicularly. We also study the case for wave optics, i.e., an incident Gaussian beam interacts with the black hole. The field pattern is plotted in Fig. 2(d), where we can see that the wave will be absorbed in the middle part, while those outside the photon sphere could escape and will interfere with each other at the opposite site. For simplicity, the above simulations are performed in two dimensions. Obviously, our model could, at least in the optical system, commendably mimic the real effects of general relativity. It is because our equivalent isotropic refractive index profile is calculated directly from the metric formula of the corresponding space that the property of the analog space can be well maintained.

To visualize the appearance of the refractive-index profile given in Eq. (7), we have added to our scientific ray tracer Dr TIM [33] the capability to trace rays in transformation-optics media. A fourth-order Runge-Kutta algorithm is used to solve the Hamilton-type equations, derived in Ref. [45], describing ray propagation in inhomogeneous transformation-optics media. Note that we can use a slightly modified refractive index profile with a same photon sphere to a Schwarzschild black hole (see Appendix B).

After confirming that Dr TIM correctly simulated a ray on the photon sphere [Fig. 3(a)], we simulated the appearance of objects, in our case small spheres, located behind the black

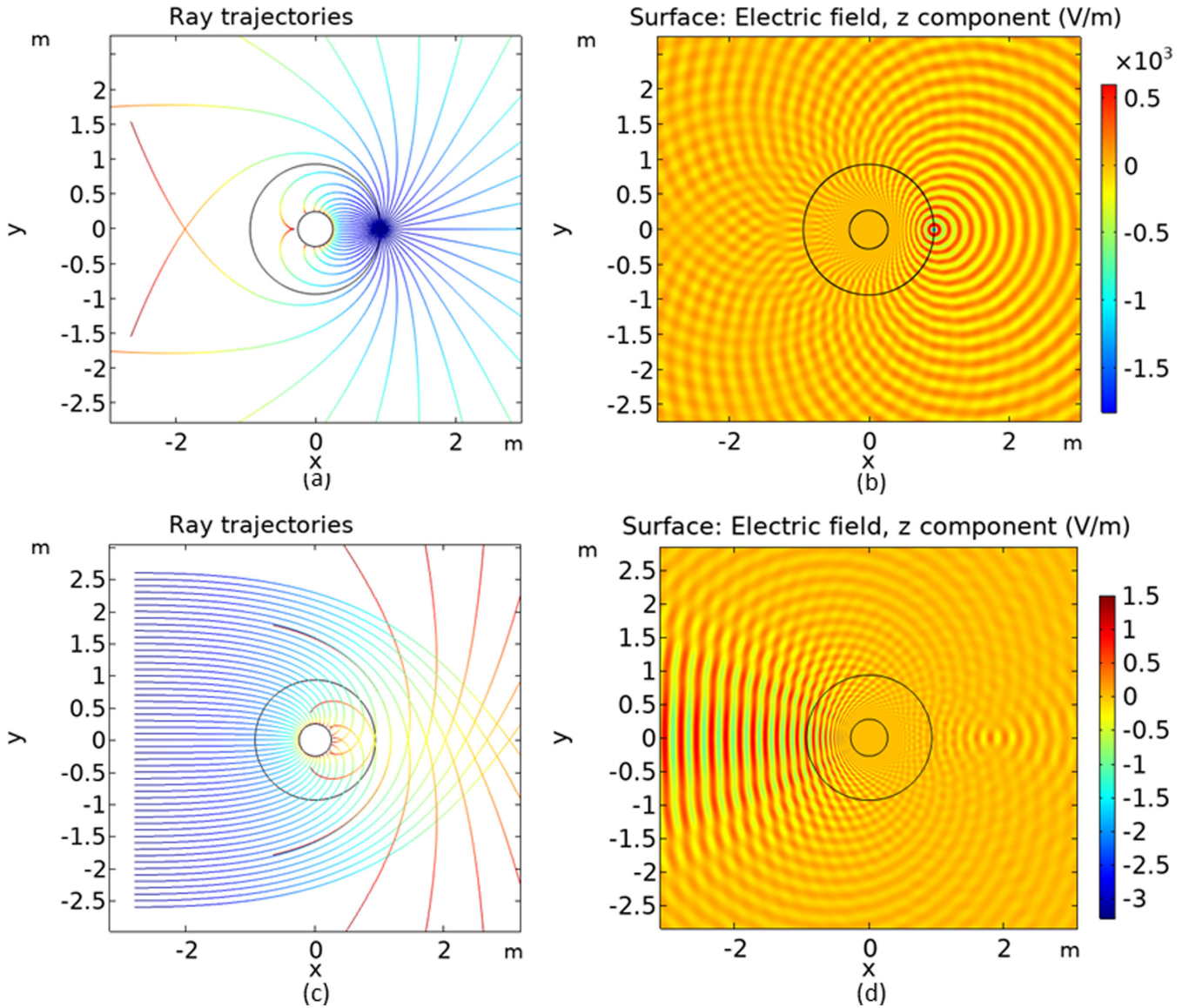


FIG. 2. A point source at the photon sphere of a black-hole lens: (a) the ray trajectories; (b) the field pattern. (c) Parallel light rays incident to the black-hole lens. (d) Gaussian beam incident to the black-hole lens.

hole [Fig. 3(c)]. In complete analogy to the Einstein rings, these small spheres become distorted into rings [Fig. 3(b)]. Finally, Fig. 3(d) shows the appearance of a scene containing a 3D lattice partially seen through a sphere filled with the refractive index distribution. The image of the lattice and the space around it shows a strong rotation and distortion, which not only reveals the gravitational-lensing effect but also leaves us some hints on investigating the objects near the black hole. This gravitational-lensing effect for an approximation of a refractive index profile in the infinity is also discussed in Appendix C.

### III. CONCLUSION

In conclusion, based on general relativity in electrical engineering and transformation optics, we propose a series of radial spatial mappings to get the equivalent isotropic refractive index profiles directly from the metric formulas

of some static spaces in general relativity. We find that the equivalent lens of de Sitter space is exactly Poincaré disk and also similar to a zero index lens, while that of anti-de Sitter space is simply Maxwell's fish-eye lens. In particular, we analyze a previous version of optical black hole and find that it has infinite photon spheres, while our black hole only has a unique photon sphere, which is the reason for the famous donutlike halo of a realistic black hole. We study the light behavior and wave pattern in the de Sitter space and outside the black hole both from geometrical optics and wave optics. We could realize the black-hole halo by 2D figures with the source of a point or some parallel light rays (Gaussian beam). Most importantly, with the isotropic refractive index profile in hand, we utilize our Dr TIM to visualize the black hole. The scenes not only indicate the ray trajectories outside the event horizon and that on the photon sphere, but also present the gravitational-lensing effect and Einstein's rings around the event horizon. Moreover, we can see the image of a 3D lattice

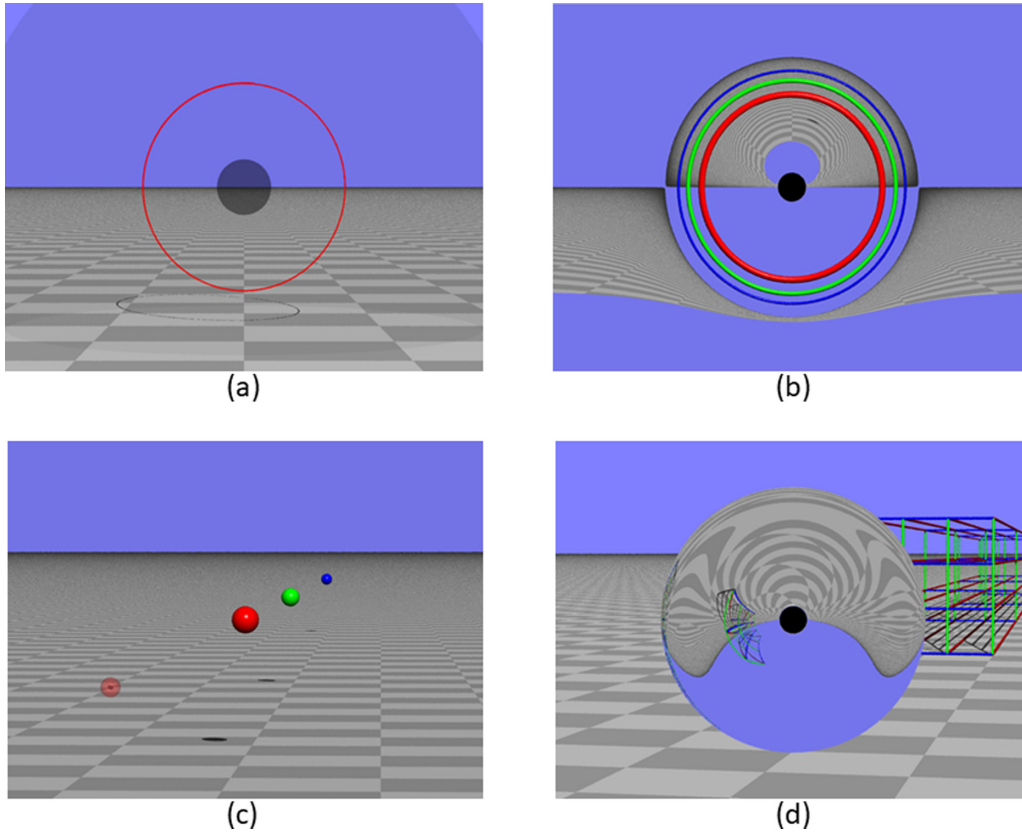


FIG. 3. Visualization using rendering ray tracing of the appearance of the artificial black hole. (a) Two orbits of a ray trajectory (red line) on the photon sphere. The event horizon is indicated by a gray sphere in the center. (b) Small spheres placed behind the black hole appear as rings. The geometry of the setup is shown in (c), with the event horizon indicated as a small gray sphere inside a semitransparent red sphere that indicates the photon sphere. (d) Simulation of a scene containing a 3D lattice seen through a sphere of radius 1 filled with the refractive index distribution. The horizon radius is 0.2 in (a) and 0.01 in (b)–(d). In (b), the refractive index distribution was simulated in a sphere of radius 5 ( $n = 1.008$  on the edge).

through the black-hole lens intuitively as a viewpoint of an observer opposite the lattice. These images could enhance our understanding of black hole and maybe we could find some new objects around the black hole according to the images. Hence, by further combining transformation optics and electrical general relativity, we could visualize a series of spaces, cosmic phenomena, or some hypothetical concepts using Dr TIM for future research, such as artificial wormholes [46,47]. This effect can be considered as electromagnetic phenomena (lensing effect). In fact, we exactly mimic the famous spaces by using their equivalent materials in the framework of electromagnetism based on the transformation optics method. The similar effects of 4D space-times are also worth studying in the future.

#### ACKNOWLEDGMENTS

This work was supported by the National Science Foundation of China (Grant No. 11874311) and the Fundamental Research Funds for the Central Universities (Grant No. 20720170015). J.B. was supported by the UK's Engineering and Physical Sciences Research Council (Grant No. EPN509668/1). R.-X.M. was supported by the funding of Sun Yat-Sen University.

#### APPENDIX A: THE UNIQUE PHOTON SPHERE OF THE REFRACTIVE INDEX PROFILE, EQ. (7)

Consider a light ray in a medium described by isotropic metric  $g_{ij}$  [expressed in spherical coordinates  $(r, \theta, \phi)$ ]

$$g_{ij} = n^2(r) \times \text{diag}(1, r^2, r^2 \sin^2 \theta). \quad (\text{A1})$$

Since the space described by such a metric is isotropic, the problem is effectively two dimensional, which enables us to make a choice  $\theta = \pi/2$ . The light-ray trajectory  $(r(\lambda), \pi/2, \phi(\lambda))$ , parametrized by  $\lambda$ , then satisfies the geodesic equations

$$\dot{\phi} = \frac{L}{n^2(r)r^2}, \quad (\text{A2})$$

$$\ddot{r} = \left[ 1 + \frac{r}{n(r)} \frac{dn(r)}{dr} \right] \frac{L^2}{n^4(r)r^3} - \dot{r}^2 \frac{1}{n(r)} \frac{dn(r)}{dr}, \quad (\text{A3})$$

where  $\dot{\phi} = d\phi/d\lambda$ ,  $\dot{r} = dr/d\lambda$ , and  $L$  is a constant. Light-ray trajectories in a medium with refractive index profile  $n(r)$  given by the formula

$$n(r) = \frac{(r + R_{KB})^3}{r^2(r - R_{KB})} \quad (\text{A4})$$

follow similar geodesic equations to those around a Schwarzschild black hole, i.e., a black hole described by Schwarzschild metric and  $R_{KB} = \frac{L}{4}$  in the main text [Eq. (7)]. One of the features of a Schwarzschild black hole is the *photon sphere*, a location where the light rays can travel in circles. The radius  $q$  of a “photon sphere” in a medium  $n(r)$  can be found as following: on the photon sphere,  $\dot{r} = \ddot{r} = 0$ . This is satisfied if and only if the square bracket in Eq. (A3) equals zero for  $r = q$ , i.e.,

$$1 + \frac{q}{n(q)} \frac{dn}{dr} \Big|_{r=q} = 0. \quad (\text{A5})$$

If one inserts refractive index profile  $n(r)$ , given by Eq. (A4), into Eq. (A5), the following equation is obtained:

$$\frac{q^2 - 4qR_{KB} + R_{KB}^2}{q^2 - R_{KB}^2} = 0 \quad (\text{A6})$$

when solved for  $q$ ,

$$q = R_{KB}(2 + \sqrt{3}) \quad (\text{A7})$$

#### APPENDIX B: A MODIFIED REFRACTIVE INDEX PROFILE TO OBTAIN A SAME PHOTON SPHERE OF A SCHWARZSCHILD BLACK HOLE

The radius of a photon sphere around a Schwarzschild black hole equals  $3R/2$ . This discrepancy can be fixed by inserting a parameter  $j$  to formula (A4) as follows:

$$n_{KB}(r) = \frac{(r + jR)^3}{r^2(r - R)}. \quad (\text{B1})$$

For such a distribution, the radius  $q$  of a photon sphere equals

$$q = R(j + 1 + \sqrt{(j + 1)^2 - j}) \quad (\text{B2})$$

To satisfy a requirement  $q = 3R/2$ , one can solve Eq. (B2) for  $j$ , yielding a value  $j = -3/8$ .

#### APPENDIX C: GRAVITATIONAL-LENSING EFFECT FOR AN APPROXIMATION OF REFRACTIVE INDEX PROFILE IN INFINITY

At distance  $r$  much larger than the Schwarzschild radius  $R_S$ , i.e., if  $r \gg R_S$ , the space-time around a Schwarzschild black hole can be approximated by a refractive index distribution  $n_S(r)$ ,

$$n_S(r) = 1 + 2\frac{R_S}{r} \quad (\text{C1})$$

If a light ray, traveling from infinity, passes around the black hole at distance  $b$ , it will be deflected by an angle  $\Delta\theta(b)$ ,

$$\Delta\theta(b) = 2\frac{R_S}{b}. \quad (\text{C2})$$

If a light source is placed exactly behind the lensing black hole at distance  $D_{SL}$  from that black hole, an observer at distance  $D_L$  will observe a ring around the black hole of an Einstein’s radius, with a characteristic angle  $\theta_E$ :

$$\theta_E = \sqrt{2R_S \frac{D_{SL}}{(D_{SL} + D_L)D_L}}. \quad (\text{C3})$$

Very similar results can be obtained with our index profile given by Eq. (B1). For  $r \gg R$ , the refractive index profile can be approximated:

$$n_{KB}(r) \approx 1 + 2\frac{\frac{3j+1}{2}R}{r}. \quad (\text{C4})$$

This implies that one can simply substitute  $R_S \rightarrow (3j + 1)R/2$  to the formulas well known for weak gravitational lensing and obtain the correct values.

- 
- [1] A. Einstein, Approximative integration of the field equations of gravitation[J], Sitzungsber. K. Preuss. Akad. Wiss., **1**, 688 (1916).
- [2] B. P. Abbott *et al.*, Observation of Gravitational Waves from a Binary Black Hole Merger, *Phys. Rev. Lett.* **116**, 061102 (2016).
- [3] K. Akiyama *et al.* (The event horizon telescope collaboration), First M87 Event Horizon Telescope Results. I. The Shadow of the Supermassive Black Hole, *Astrophys. J. Lett.* **875**, L1 (2019).
- [4] U. Leonhardt and T. G. Philbin, General relativity in electrical engineering, *New J. Phys.* **8**, 247 (2006).
- [5] U. Leonhardt, Optical conformal mapping, *Science* **312**, 1777 (2006).
- [6] J. B. Pendry, D. Schurig, and D. R. Smith, Controlling electromagnetic fields, *Science* **312**, 1780 (2006).
- [7] M. McCall, J. B. Pendry, V. Galdi, Y. Lai, S. A. R. Horsley, J. Li, J. Zhu, R. C. M. Thomas, O. Q. Teruel, P. Tassin, V. Ginis, E. Martini, G. Minatti, S. Maci, M. Ebrahimpouri, Y. Hao, P. Kinsler, J. Gratus, J. M. Lukens, A. M. Weiner, U. Leonhardt, I. I. Smolyaninov, V. N. Smolyaninova, R. T. Thompson, M. Wegener, M. Kadic, and S. A. Cummer, Roadmap on transformation optics, *J. Opt.* **20**, 063001 (2018).
- [8] H. Chen and C. Chan, Transformation media that rotate electromagnetic fields, *Appl. Phys. Lett.* **90**, 241105 (2007).
- [9] H. Chen, B. Hou, S. Chen, X. Ao, W. Wen, and C. Chan, Design and Experimental Realization of a Broadband Transformation Media Field Rotator at Microwave Frequencies, *Phys. Rev. Lett.* **102**, 183903 (2009).
- [10] M. Rahm, D. Schurig, D. A. Roberts, S. A. Cummer, D. R. Smith, and J. B. Pendry, Design of electromagnetic cloaks and

- concentrators using form-invariant coordinate transformations of Maxwell's equations, *Photonic Nanostruct.* **6**, 87 (2008).
- [11] C. Y. Li, L. Xu, L. L. Zhu, S. Y. Zou, Q. H. Liu, Z. Y. Wang, and H. Chen, Concentrators for Water Waves, *Phys. Rev. Lett.* **121**, 104501 (2018).
- [12] D. Shurig, J. B. Pendry, and D. R. Smith, Transformation-designed optical elements, *Opt. Express* **15**, 14772 (2007).
- [13] U. Leonhardt and T. G. Philbin, Perfect imaging with positive refraction in three dimensions, *Phys. Rev. A* **81**, 011804(R) (2010).
- [14] V. Ginis, P. Tassin, J. Danckaert, C. M. Soukoulis, and I. Veretennicoff, Creating electromagnetic cavities using transformation optics, *New J. Phys.* **14**, 033007 (2012).
- [15] H. Y. Chen, R.-X. Miao, and M. Li, Transformation optics that mimics the system outside a Schwarzschild black hole, *Opt. Express* **18**, 15183 (2010).
- [16] S. S. Hegde and C. V. Vishveshwara, Optical analogues of spherically symmetric black hole spacetimes, *J. Phys.: Conf. Ser.* **484** 012017 (2014).
- [17] V. Ginis, P. Tassin, B. Craps, and I. Veretennicoff, Frequency converter implementing an optical analogue of the cosmological redshift, *Opt. Express* **18**, 5350 (2010).
- [18] M. Li, R.-X. Miao, and Y. Pang, Casimir energy, holographic dark energy and electromagnetic metamaterial mimicking de Sitter, *Phys. Lett. B* **689**, 55 (2010).
- [19] M. Li, R.-X. Miao, and Y. Pang, More studies on metamaterials mimicking de Sitter space, *Opt. Express* **18**, 9026 (2010).
- [20] S.R. Boston, Time travel in transformation optics: Metamaterials with closed null geodesics, *Phys. Rev. D* **91**, 124035 (2015).
- [21] T. G. Mackay and A. Lakhtakia, Towards a realization of Schwarzschild-(anti-)de Sitter spacetime as a particulate metamaterial, *Phys. Rev. B* **83**, 195424 (2011).
- [22] D. A. Genov, S. Zhang, and X. Zhang, Mimicking celestial mechanics in metamaterials, *Nat. Phys.* **5**, 687 (2009).
- [23] E. E. Narimanov and A. V. Kildishev, Optical black hole: Broadband omnidirectional light absorber, *Appl. Phys. Lett.* **95**, 041106 (2009).
- [24] C. Argyropoulos, E. Kallos, and Y. Hao, FDTD analysis of the optical black hole, *J. Opt. Soc. Am. B* **27**, 2020 (2010).
- [25] Q. Cheng, T. J. Cui, W. X. Jiang, and B. G. Cai, An omnidirectional electromagnetic absorber made of metamaterials, *New J. Phys.* **12**, 063006 (2010).
- [26] C. Sheng, H. Liu, Y. Wang, S. N. Zhu, and D. Genov, Trapping light by mimicking gravitational lensing, *Nat. Photonics* **7**, 902 (2013).
- [27] C. Sheng, R. Bekenstein, H. Liu, S. N. Zhu, and M. Segev, Wavefront shaping through emulated curved space in waveguide settings, *Nat. Commun.* **7**, 10747 (2016).
- [28] C. Sheng, H. Liu, H. Y. Chen, and S. N. Zhu, Definite photon deflections of topological defects in metasurfaces and symmetry-breaking phase transitions with material loss, *Nat. Commun.* **9**, 4271 (2018).
- [29] V. Perlick, On Fermat's principle in general relativity: I. The general case, *Classical Quantum Gravity* **7**, 1319 (1990).
- [30] V. Perlick, On Fermat's principle in general relativity: II. The conformally stationary case, *Classical Quantum Gravity* **7**, 1849 (1990).
- [31] M. Šarbot and T. Tyc, Spherical media and geodesic lenses in geometrical optics, *J. Opt.* **14**, 075705 (2012).
- [32] L. Xu, X. Y. Wang, T. Tyc, C. Sheng, S. N. Zhu, H. Liu, and H. Y. Chen, Light rays and waves on geodesic lenses, *Photonics Res.* **7**, 1266 (2019).
- [33] S. Oxburgh, T. Tyc, and J. Courtial, Dr TIM: Ray-tracer TIM, with additional specialist scientific capabilities, *Comput. Phys. Commun.* **185**, 1027 (2014).
- [34] A. Cvetkovski and M. Crovella, Multidimensional scaling in the Poincaré disk, *Appl. Math. Inf. Sci.* **10**, 125 (2016).
- [35] É. Ghys, Poincaré and his disk, The scientific legacy of Poincaré, **36**, 17 (2006).
- [36] Q. Cheng, W. X. Jiang, and T. J. Cui, Spatial Power Combination for Omnidirectional Radiation via Anisotropic Metamaterials, *Phys. Rev. Lett.* **108**, 213903 (2012).
- [37] J. C. Maxwell, Solutions of problems, *Cambridge Dublin Math. J.* **8**, 188 (1854).
- [38] S. Khorasani and B. Rashidian, Optical anisotropy of Schwarzschild metric within equivalent medium framework, *Opt. Commun.* **283**, 1222 (2010).
- [39] R. Doran, F. S. N. Lobo, and P. Crawford, Interior of a Schwarzschild black hole revisited, *Found. Phys.* **38**, 160 (2008).
- [40] H. Kawai and Y. Yokokura, Interior of black holes and information recovery, *Phys. Rev. D* **93**, 044011 (2016).
- [41] L. Xu and H. Y. Chen, Conformal transformation optics, *Nat. Photonics* **9**, 15 (2015).
- [42] U. Leonhardt and T. Philbin, *Geometry and Light: The Science of Invisibility* (Courier Corporation, Chelmsford, MA, 2012).
- [43] J. E. Eaton, On spherically symmetric lenses, *Trans. IRE Antennas Propag.* **PGAP-4**, 66 (1952).
- [44] A. J. Danner and U. Leonhardt, Lossless design of an Eaton lens and invisible sphere by transformation optics with no bandwidth limitation, in International Quantum Electronics Conference (Optical Society of America, 2009).
- [45] D. Schurig, J. B. Pendry, and D. R. Smith, Calculation of material properties and ray tracing in transformation media, *Opt. Express* **14**, 9794 (2006).
- [46] A. Greenleaf, M. Lassas, and G. Uhlmann, Electromagnetic Wormholes and Virtual Magnetic Monopoles from Metamaterials, *Phys. Rev. Lett.* **99**, 183901 (2007).
- [47] J. Zhu, Y. Liu, Z. Liang, T. Chen, and J. Li, Elastic Waves in Curved Space: Mimicking a Wormhole, *Phys. Rev. Lett.* **121**, 234301 (2018).